ENHANCING HEAT TRANSFER IN A THERMAL STORAGE UNIT WITH SYMMETRICALLY ARRANGED CURVED FINS

Xin GU, Hanzhen WANG, Jie WANG, Weijie CHEN, Jinting ZHANG, Yongqing WANG*

School of Mechanical and Power Engineering, Zhengzhou University, Zhengzhou 450001, China
* Corresponding author, E-mail address: wangyq@zzu.edu.cn

Phase change materials (PCMs) offer a promising solution to the imbalance between energy supply and demand by storing latent heat. However, their low thermal conductivity limits their widespread application. To enhance heat storage efficiency, a triplex-tube heat storage unit was proposed with symmetrically arranged curved fins, and its performance was compared with that of a traditional straight-fin unit. The melting process within a triplex-tube system containing various curved fin arrangements was investigated. The results indicate that curved fins yield a stronger heat transfer effect in specific regions compared to straight fins. However, the inherent asymmetry of conventionally arranged curved fins reduces overall heat transfer efficiency. The symmetrically arranged curved fins demonstrate the potential to provide stronger convective heat transfer and a more uniform temperature distribution. Compared to straight-fin heat storage units, the melting speed of symmetrically arranged curved-fin units increases by 9.1% to 13.8%, and the average charging power increases by 10.3% to 14.1%. The fin configurations and enhancement methods offer a novel approach to fin optimization in thermal storage units.

Keywords: *Phase change material, Symmetrically arranged curved fins, Latent heat thermal energy storage*

1. Introduction

The excessive consumption of non-renewable energy sources has resulted in the depletion of fossil fuels and a worsening greenhouse effect. In response, there is an active global pursuit of cleaner, renewable energy alternatives. Solar energy, with advantages of abundance, environmental benefits, and sustainability, stands out as a prominent option [1]. However, the intermittent nature of solar power poses a challenge, as its availability does not consistently match energy demand. Thermal energy storage (TES) emerges as a viable solution to mitigate this issue [2]. Among various TES technologies, latent heat thermal energy storage (LHTES), which utilizes phase change materials (PCMs), has gained significant attention due to its high energy storage density and ability to maintain stable temperatures during the storage process. Beyond solar energy applications [3], LHTES has found utility in multiple fields, such as battery thermal management, building energy conservation, and waste heat recovery [4, 5]. The principal obstacle hindering the widespread adoption of LHTES systems is the inherent low thermal conductivity of PCMs.

The addition of fins significantly increases the heat transfer area, and their installation and maintenance are relatively straightforward. This approach represents the most cost-effective method

for enhancing the heat transfer efficiency of LHTES systems. Various fin configurations, including annular, rectangular, spiral, corrugated, tree-shaped, and fractal geometries [6–8], have been explored. Rathod et al. [9] experimentally demonstrated that incorporating longitudinal rectangular fins on the heat exchange tubes of an LHTES system reduce the solidification time by 43.6%. Similarly, Yan et al. [10] enhanced a LHTES system with Y-shaped fins to improve heat transfer, finding that decreasing fin thickness and increasing fin angle effectively accelerate the melting of the PCM. Inspired by natural snowflakes, Zhang et al. [11] designed snowflake fins and demonstrated a remarkable 32.23% to 51.81% reduction in total melting and solidification time compared to straight fins. In a double-tube LHTES system, Boujelbene et al. [12] compared the performance of spiral and straight fins, observing that spiral fins exhibited superior performance with a 10% and 14% increase in charging and heat discharge rates, respectively. In another study, Mao et al. [13] developed a vertical pointer-shaped fin by combining rectangular and triangular fins. Their study revealed that pointer-shaped fins reduce the melting time of PCMs by 15.1% compared to rectangular fins. Nie et al. [14] investigated the impact of helm-shaped fins on the solidification performance of PCMs in vertical double-tube heat storage units, and their results indicated that the optimal heat transfer enhancement of helm-shaped fins was achieved. Yao et al. [15] optimized the melting performance of a triplex-tube TES system using V-shaped fins, finding that the optimal V-shaped fin configuration, compared to rectangular fins, led to a substantial 31.92% reduction in melting time.

Furthermore, researchers have investigated the impact of curved fins on the performance of LHTES system. Palmar et al. [16] showed that curved fins provide a better fit with round tube heat storage units compared to straight fins. Tavakoli et al. [17] demonstrated that optimizing the dimensions of sinusoidal curved fins in the heat storage unit can result in a 62% increase in charging speed compared to straight fins. Iranmanesh and Moshizi [18] conducted a study examining the parameters of sinusoidal fins in a triplex-tube heat storage unit. Their findings indicated that a configuration with an amplitude of 5 mm and a wavelength of 25 mm exhibited optimal performance in both the melting and solidification phases. Kumar et al. [19] discovered that devices with wavy fins released energy at a faster rate than those with straight fins when operating at higher speeds. Guo et al. [20] observed that incorporating concave fins into rectangular heat storage units can facilitate convective heat transfer during a defined melting period.

The aforementioned studies demonstrate that incorporating fins can effectively enhance the performance of LHTES system. However, the introduction of curved fins into circular heat storage units creates asymmetry within the latent heat thermal energy storage system, and the implications of which on system performance require further investigation. Therefore, this paper aims to improve the heat transfer and melting characteristics of PCM by optimizing the arrangement of curved fins. The objective is to significantly enhance the melting and heat transfer performance of latent heat thermal energy storage systems, thereby promoting their advancement and practical application.

2. Research model and numerical method

2.1. Research model

The LHTES system employed in this study adopts a horizontal triplex-tube configuration, with a PCM situated within the middle tube. This LHTES system design enables the PCM to exchange heat with both the inner and outer tubes simultaneously, thereby increasing the phase change material's heat exchange area compared to shell-and-tube LHTES systems [21]. Fig. 1(a) presents a cross-section of the LHTES used in this study. The system comprises three concentric tubes, each measuring 500 mm in length. The inner, middle, and outer tubes have diameters of 50.8 mm, 150 mm, and 200 mm, and thicknesses of 1.2 mm, 2 mm, and 2 mm, respectively. The size is chosen to ensure compatibility with solar heat exchangers [19]. Water, the selected heat transfer fluid (HTF), flows through the inner and outer tubes, serving as heat transfer channels. The annular space filled with the PCM contains eight evenly distributed fins. Fig. 1(b) depicts the computational domain structure, and the specific parameters are presented in Tab. 1. Given that the axial flow variation of the system is considerably smaller than that of the circumferential flow, the model is simplified to two dimensions [10]. It is important to note that to maintain the same PCM volume, the fin thicknesses (b) are adjusted to 1 mm, 0.98 mm, and 0.96 mm for the full straight fin, four curved fins, and eight curved fins, respectively.

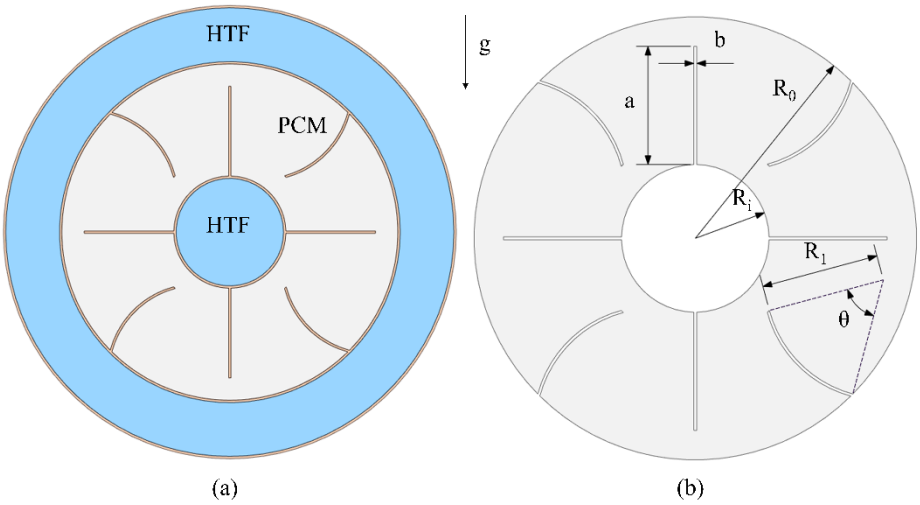

Fig. 1. Triplex-tube storage system (a) physical model and (b) computational domain

Tab. 1. Structural parameters

Parameters	R_0 [mm]	R_i [mm]	a [mm]	R_1 [mm]	θ [°]	b [mm]
Value	75	25.4	40	40	60	1/0.98/0.9

the influence of different fin arrangements on the melting performance of LHTES is primarily investigated. A total of 7 models are considered and illustrated in Fig. 2. These models are categorized based on fin arrangement. The reference model (RM) employs straight fins. The CM1-CM3 models utilize conventionally arranged curved fins. The SM1-SM3 models feature symmetrically arranged curved fins.

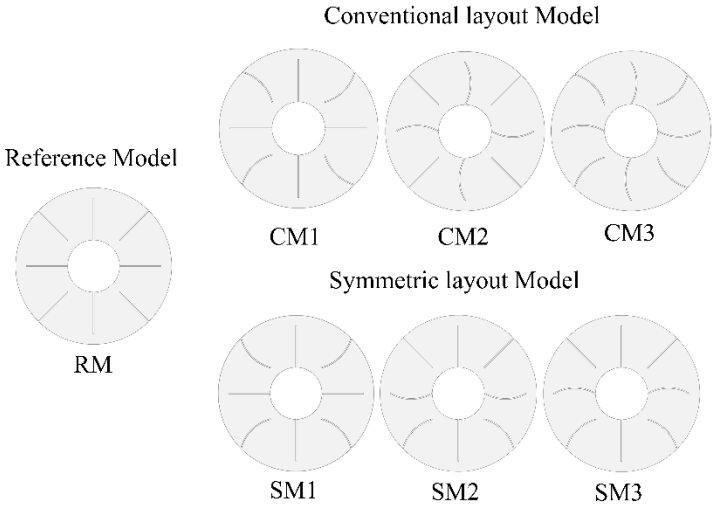

Fig. 2. Classification of calculation models

2.2. Thermal properties of materials

In this paper, the LHTES system uses RT35 as the PCM and copper for the fin and tube wall material. The materials' thermophysical properties are listed in Tab. 2. RT35 was selected due to its thermal stability during phase change cycles and chemical inertness [22].

Tab. 2. Properties of materials [22]

Properties	RT35	Copper (Fin)
T_S [K]	302.15	--
T_L [K]	309.15	--
ρ [kg·m^{-3}]	770	8978
c_p [kJ·kg^{-1}·K^{-1}]	2	0.381
L [kJ·kg^{-1}]	160	--
k [W·m^{-1}·K^{-1}]	0.2	387.6
μ [Pa·s]	0.023	--
β [K^{-1}]	0.0006	--

2.3. Governing equations

The melting and solidification processes of the PCM are simulated using the enthalpy-porosity model developed by Voller and Prakash [23]. To simplify the calculation process, the following assumptions are made: (1) The liquid phase change material exhibits transient, laminar, and incompressible flow [7]. (2) The temperature change of the HTF is negligible [11]. (3) The thermal properties of the phase change material remain constant within the working temperature range, and the density change of the phase change material is approximated using the Boussinesq approximation [18]. (4) Volume change, viscous dissipation, heat loss from the outer wall, and radiative heat transfer during the phase change process are negligible [24].

Considering the aforementioned assumptions, the governing equations for fluid flow and heat transfer are presented as follows:

Continuity equation:

$$\frac{\partial \rho}{\partial t} + \nabla \cdot \vec{U} = 0 \tag{1}$$

Momentum equation:

$$\frac{\partial \rho \vec{U}}{\partial t} + \vec{U} \cdot \nabla \rho \vec{U} = -\nabla p + \nabla \cdot \left(\mu \nabla \vec{U} \right) + \rho g \beta (T - T_{ref}) - \frac{(1-\lambda)^2}{\lambda^3 - 0.001} A_m \vec{U} \tag{2}$$

Energy equation:

$$\frac{\partial \rho H}{\partial t} + \vec{U} \cdot \nabla \rho H = \nabla \cdot (k \bigtriangledown T) \tag{3}$$

where the mushy zone parameter A_m is typically set to a value between 10^5 and 10^8 [24]. In the study, the mushy zone parameter A_m is assumed to be 10^6. H in Eq. (3) is calculated as the sum of the sensible and latent enthalpy.:

$$H = h_{ref} + \int_{T_0}^{T} c_p \Delta T + \lambda L \tag{4}$$

The liquid fraction of the PCM, λ, is determined by the following equation:

$$\lambda = \begin{cases} 0 & T < T_s \\ \dfrac{T - T_s}{T_l - T_s} & T_s < T < T_l \\ 1 & T > T_l \end{cases} \tag{5}$$

2.4. Boundary conditions and simulation methods

The initial temperature of the PCM region is set at 288.15 K, below the PCM's phase change temperature, ensuring that the PCM remains in a solid state. The PCM is heated using water at a temperature of 323.15 K, and all walls are subjected to no-slip boundary conditions. The software ANSYS Fluent was employed for the numerical simulations. The governing equations were discretized using the finite volume method (FVM), and the pressure-velocity coupling was handled using the SIMPLE algorithm. The pressure correction equation was solved in PRESTO! format. The QUICK differencing scheme was adopted for the discretization of convective terms in the momentum and energy equations. The convergence criteria were set to 10^{-4} for the continuity and momentum equations, and to 10^{-8} for the energy equation.

3. Independency study and model validation

To ensure the grid and time step independence of the simulation results, the straight-fin model was subjected to grid and time step independence tests. Four grid schemes, with grid number of 13346, 30856, 48207, and 85618, were employed to investigate the variation of the liquid fraction over time, as shown in Fig. 3(a). As illustrated in Fig. 3(a), a grid with grid number of 48207 is sufficient to achieve the desired accuracy, and further grid refinement does not significantly alter the results. The time step was verified using 0.5 s, 0.1 s, and 0.05 s, as depicted in Fig. 3(b). With a time

step of 0.1 seconds, the iterative process achieved full convergence, and the results were essentially identical to those obtained with a time step of 0.05 seconds. To ensure both the accuracy and efficiency of the simulation, a grid number of 48207 and a time step of 0.1 s were selected for the numerical scheme.

Furthermore, the present findings were compared with the experimental data reported by Al-Abidi et al. [25]. In their study, a triplex-tube heat exchanger with internal and external fins was employed, using RT82 as the PCM and water as the HTF. The HTF inlet temperature was maintained at 363.15 K, and the PCM, initially at room temperature, was heated. To monitor the average temperature during the phase change process, 15 temperature measurement points were placed within the PCM. The present numerical simulation employed identical boundary conditions to those used in the experimental study. Fig. 3(c) presents a comparison of the mean temperature evolution over time for both studies. As depicted in Fig. 3(c), the data obtained from the simulation model agree well with the experimental data, thus validating the accuracy and reliability of the current model and method.

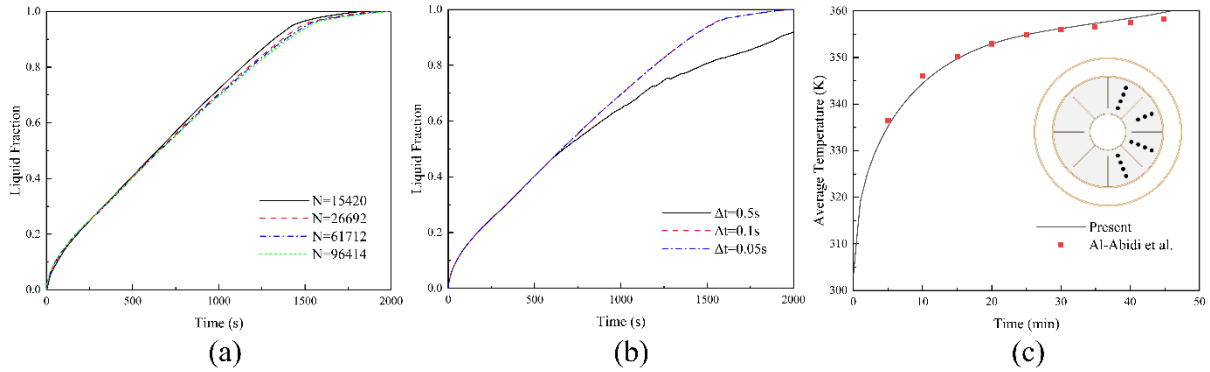

Fig. 3. (a) Grid and (b) time step independences study; and (c) Comparison of the average temperature with the experimental data from the literature

4. Results and discussion

4.1. Effects of conventionally arranged curved fins on melting performance

Fig. 4 present the liquid fraction contours and isotherms at different times for the three conventional curved fin models (CM1, CM2, CM3) and the reference model (RM). At *t* of 5 min, the liquid fraction contours of the four models exhibit a high degree of similarity, with the liquid PCM uniformly distributed along the wall and fins. At this stage, heat conduction dominates heat transfer. As the process continues, heat is gradually transmitted through the PCM, leading to an increase in the liquid PCM. Buoyancy forces act on some of the liquid PCM, causing it to move upwards and initiate natural convection. At this point, the prevailing heat transfer transitions from conduction to convection. The convective motion accelerates the melting of the upper portion of each region delineated by the fins. Consequently, the liquid PCM gradually occupies the majority of the available space (t = 30 min). The heated fluid flows through the upper part of the annular space, causing the upper region to melt completely first. The fins positioned diagonally below the annular space impede the upward flow of liquid PCM, creating a slow-melting zone in this region. Consequently, the dominant heat transfer mechanism at the solid-liquid interface reverts to conduction. This phenomenon continues until the melting process is complete. Additionally, during the late melting phase, the slow

melting zones on the left side of CM1 and the right side of CM2 are smaller than those in RM. This suggests that the curved-fins effectively enhance the melting rate of PCM in specific regions.

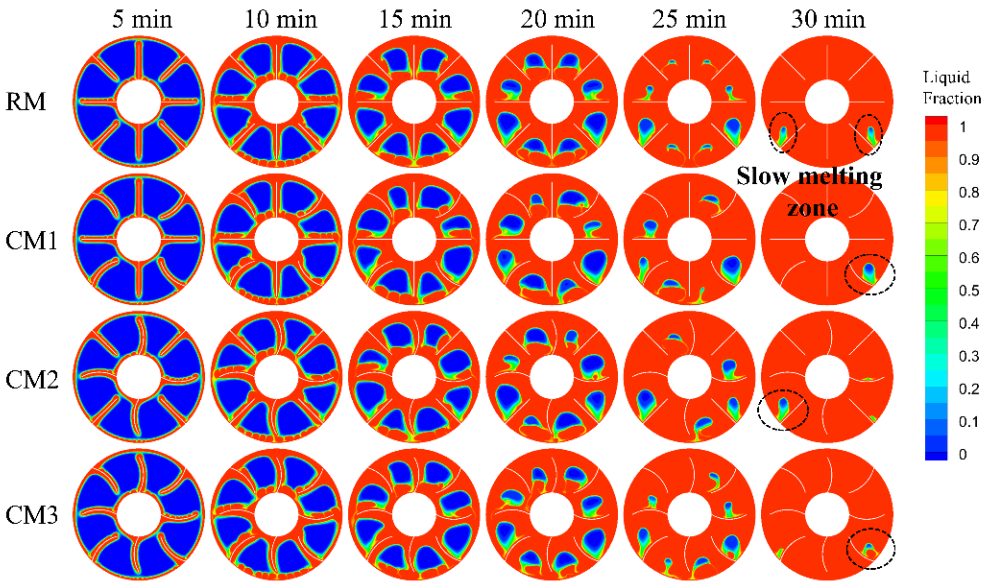

However, the accumulation of solid PCM on the opposite side reduces the overall melting rate of the LHTES system.

Fig. 4. Liquid fraction contours in the straight-fin and the conventionally arranged curved fin models

Fig. 5(a) shows the evolution of the liquid fraction for the reference model (RM) and the three conventionally arranged curved-fin models (CM1, CM2, and CM3). Fig. 5(b) presents the evolution of the difference in liquid fraction between conventionally arranged curved-fin models and RM. The complete melting time for RM is 33.5 min, while CM1 and CM2 extend melting times of 35.9 and 35.1 min, respectively, indicating a detrimental impact on melting performance. Among the four models, CM3 exhibits the shortest total melting time of 32.5 min, representing a 3% reduction compared to RM. At the initial stage of melting, the melting fraction of all four models shows a nearly identical trend, suggesting that heat transfer is predominantly governed by conduction. As melting progresses, convective heat transfer becomes the dominant mode, with the curved fins, designed to enhance convection, becoming increasingly influential. CM3, with the most curved fins, achieves the highest melting fraction during the intermediate phase. In the later melting phase, as convection intensity diminishes, the process reverts to being conduction-dominated. At this stage, the size of the slow-melting zone significantly impacts the overall melting rate. In the final stages, the slow-melting regions of CM1 and CM2 are concentrated on one side, a consequence of the asymmetry introduced by the curved fins. This asymmetry results in an enlarged slow-melting region, causing the total melting time of CM1 and CM2 to be longer than that of RM, despite their faster melting rates in the medium term.

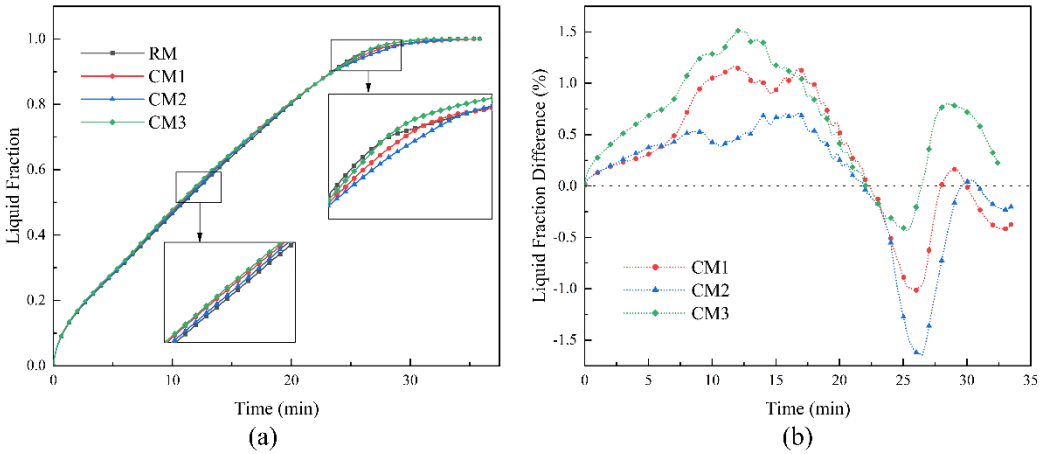

Fig. 5. Evolution of (a) liquid fraction and (b) liquid fraction difference for the conventionally arranged curved fin models and the straight fin model

To further elucidate the impact of asymmetry during the melting process, the temperature at eight points in the four models (RM, CM1, CM2, CM3) are compared. Points P1 to P4 are located on the right side of the diagram, while points P5 to P8 are situated on the left. The mean temperature of the points in the left and right groups are calculated separately, and the temporal evolution of these mean temperatures is depicted in Fig. 6. As shown in Fig. 6, the temperatures at the left point of CM1 and the right points of CM2 and CM3 are significantly higher than those of RM, indicating that the bent fin effectively enhances the heat transfer rate of PCM in specific regions. However, the temperature at the right point of CM1 and the left point of CM3 shows little difference compared to RM, and the temperature at the left point of CM2 is significantly lower than that of RM, suggesting that the bent fin has structural limitations in improving the heat transfer efficiency of PCM. The temperature differential between the left and right sides of CM2 is most pronounced at t = 24.4 min, with an average temperature difference of 7.4 K. These findings highlight the detrimental impact of the melting asymmetry, caused by the traditional curved fin arrangement, on the melting performance of the LHTES.

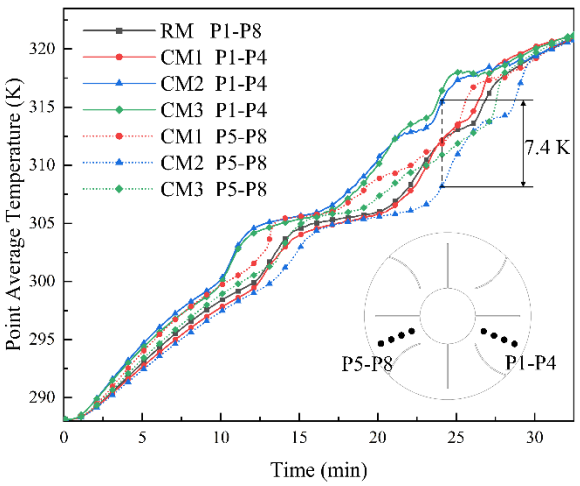

Fig. 6. Evolution of point average temperature

4.2. Effects of symmetrically arranged curved fins on melting performance

The preceding analysis demonstrates that the use of curved fins can enhance heat transfer in specific regions of the LHTES system. However, the overall effect on the system is suboptimal and may even be detrimental. This phenomenon is closely linked to the melting asymmetry caused by the conventional arrangement of the curved fins. To address this issue, the concept of symmetrically arranged curved fins is proposed and three such models (SM1, SM2, SM3) are presented for

optimizing the areas where the phase change material melts more slowly. The subsequent analysis examines the impact of these symmetrically arranged curved fins on the overall melting performance.

Fig. 7 illustrates the distribution of liquid fraction and temperature for three symmetrically arranged curved-fin models (SM1, SM2, SM3). Compared to Fig. 4, the implementation of symmetrically arranged curved fins results in a more homogeneous melting. Unlike in the conventionally arranged curved fin models, the slow-melting zone of the PCM is reduced and distributed across multiple zones in the three symmetrically arranged curved fin models. This ensures a larger heat transfer area between the solid and liquid PCM in the later stages of melting, thereby facilitating improved heat transfer. Among the three models, SM2 exhibits the largest low-temperature zone situated above the center fin. This is attributed to the substantial isolation area created by the concave curved fin in the center and the straight fin positioned diagonally above it. Additionally, the concave curved fin hinders natural convection from below and the sides, thus reducing the effectiveness of heat transfer. Replacing the middle fins with upwardly convex curved fins (SM3) effectively mitigate this phenomenon while simultaneously enhancing natural convection in the central region. Compared to SM2 and SM3, SM1 has a larger space delineated by fins at the top, which accommodates more PCM. During the melting phase, the liquid PCM flows upwards in the container due to natural convection, and the solid PCM at the top provides the conditions for sustained convective heat transfer. Therefore, SM1 exhibits the greatest capacity for maintaining convective heat transfer, with the longest duration of natural convection during the melting process and the most uniform temperature distribution.

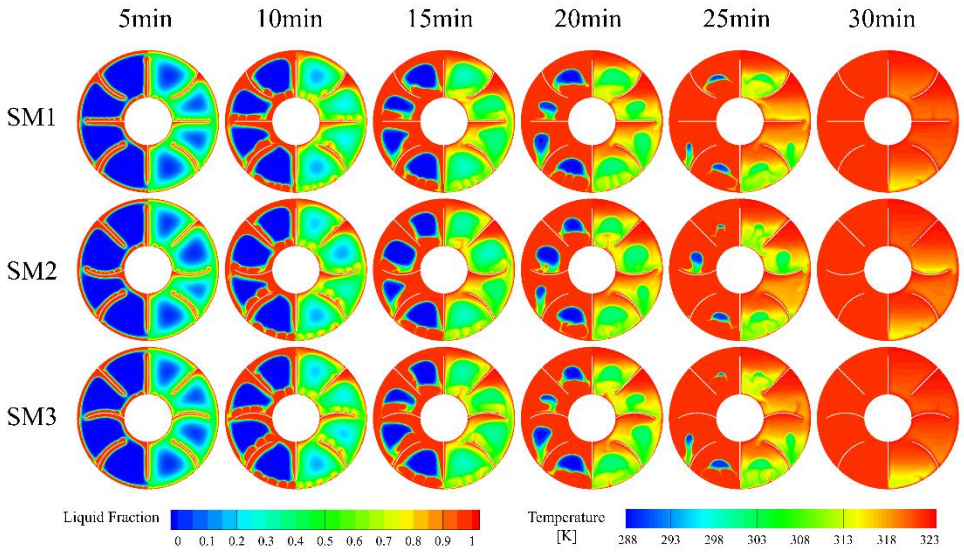

Fig. 7. Distribution of the liquid fraction (left semicircle) and temperature (right semicircle) in the symmetrically arranged curved fin models

Fig. 8(a) illustrates the evolution of the liquid fraction for the reference model (RM) and the three symmetrically arranged curved-fin models (SM1, SM2, and SM3). Fig. 8(b) shows the evolution of the difference in liquid fraction between the three symmetrically arranged curved-fin models and the RM. The complete melting times for SM1, SM2, and SM3 are 28.9 min, 30 min, and 29.4 min, respectively, representing reductions of 13.8%, 9.1%, and 12.1% compared to the RM. These results

demonstrate that symmetrically arranged curved fins effectively enhance the heat transfer performance of LHTES. Moreover, the configuration of the fins significantly influences the melting rate. Throughout the melting period, the rate for SM3 consistently surpasses that of SM2, indicating that a convex middle fin promotes stronger convection compared to a concave one. SM1 exhibits the longest duration of convective heat transfer, remaining the predominant mode throughout most of the melting process until the PCM is nearly completely melted.

Fig. 8. Evolution of (a) liquid fraction and (b) liquid fraction difference for the symmetrically arranged curved fin models and the straight fin model

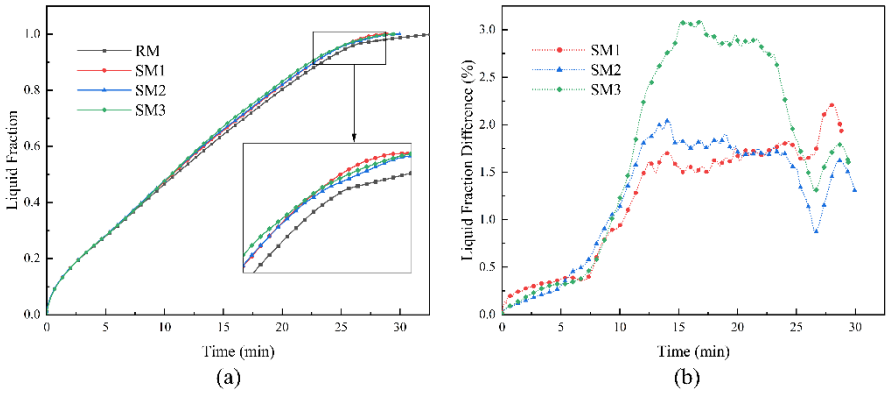

4.3 Comparison of melting performance

To facilitate a comparative analysis of the effects of different fin arrangements on the melting performance of TES systems, a percentage improvement in melting performance (PIMP) metric, denoted by σ (%), has been defined. This metric enables a quantitative comparison of the optimization effects of different structural configurations on the complete melting time of TES systems. The calculation equation for PIMP is as follows:

$$\sigma = \frac{t_{RM} - t_{OM}}{t_{RM}} \times 100\% \tag{6}$$

where t_{RM} is the total melting time of RM, and t_{OM} is the total melting time of the other models. Fig. 9 presents the complete melting times and the PIMP values for all models.

As shown in Fig.9, SM1 exhibits the most substantial enhancement in melting performance, with a 13.7% increase. The smallest improvement is observed for CM3, with a 3.0% increase. The negative σ values for CM1 and CM2 indicate that these models do not effectively enhance melting performance. Furthermore, models with symmetrically arranged curved fins exhibit a significantly higher percentage increase in melting

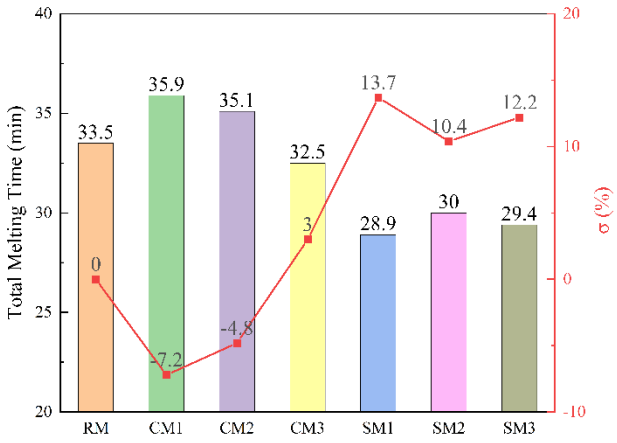

Fig. 9. Total melting time and PIMP values

performance compared to those with conventionally arranged curved fins.

Fig. 10 illustrates the transient heat transfer rate and average charging power for the seven models. The transient heat transfer rate generally demonstrates a decreasing trend across all structural configurations. This is attributed to the initial high heat transfer rate resulting from direct contact between the heating surface and the solid phase change material, which facilitates efficient heat conduction. As melting proceeds, the emergence of a liquid PCM layer adjacent to the heated surface increases the overall thermal resistance, significantly impeding the heat transfer process. Subsequently, convective heat transfer becomes the dominant mode, and the heat transfer rate gradually decreases until the phase change material is completely melted.

Fig. 10(a) depicts that the heat transfer rates of CM1, CM2, and CM3 initially exceed that of the reference model (RM) during the early melting phase. However, owing to the structural asymmetry, the heat transfer rates of CM1 and CM2 subsequently decrease, eventually falling below that of the RM in the later melting phase. Fig. 10(b) illustrates that during the initial and intermediate melting phases, the symmetrically arranged curved fin models with optimized configurations mitigate the impact of melting asymmetry and enhance the transient heat transfer rate of the TES system. As depicted in Fig. 10(c), the implementation of symmetrically arranged curved fins enhances the average charging power by 10.3% to 14.1% compared to the RM.

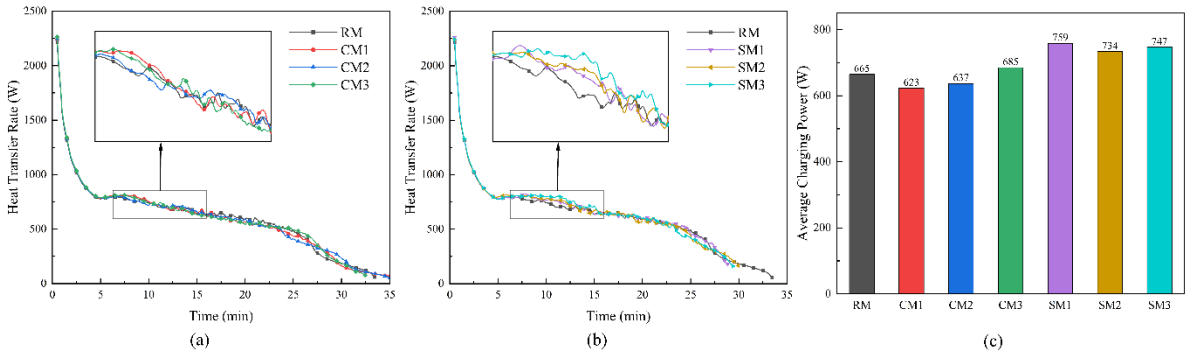

Fig. 10. Transient heat transfer rates for (a) the conventionally arranged curved fin model, (b) the symmetrically arranged curved fin model, and (d) the average charging power for all models

5. Conclusion

The impact of incorporating curved fins into a triplex-tube LHTES on its heat storage performance through numerical simulations was investigated. To further enhance the heat transfer and melting performance, a symmetrical fin arrangement is proposed. A straight-fin model serves as a reference to evaluate the effects of curved fin configurations on the thermal storage performance in a triplex-tube LHTES system. The key findings are summarized as follows:

(1) Curved fins enhance the convective heat transfer during the LHTES melting process. Nevertheless, the inherent asymmetry of conventionally arranged curved fins leads to the formation of a larger slow-melting zone on one side of the phase change material, impeding its complete melting.

(2) Due to the inherent asymmetry, the complete melting time of the fully curved fin model (CM3) is reduced by only 3% compared to the reference model, while the complete melting

times of the two semi-curved fin models (CM1 and CM2) are increased by 7.2% and 4.8%, respectively.

(3) The symmetrical arrangement of curved fins facilitates a more uniform temperature distribution and promotes stronger and more sustained convective heat transfer, thereby effectively enhancing the thermal performance of the LHTES.

(4) In the case of symmetrical arrangement, the strongest natural convection occurs in the model SM3, resulting in a 12.1% increase in melting speed and a 12.3% increase in average charging power. In contrast, the model SM1 demonstrates the longest duration of natural convection, leading to a 13.7% increase in melting speed and a 14.1% increase in average charging power.

The fin configurations and enhancement methods proposed in this study offer novel insights into the design of LHTES systems.

References

[1] Khodadadi, M., Sheikholeslami, M., Numerical simulation on the efficiency of PVT system integrated with PCM under the influence of using fins, *Solar Energy Materials and Solar Cells, 233* (2021), 111402.

[2] Yang, X., *et al*., Design and operating evaluation of a finned shell-and-tube thermal energy storage unit filled with metal foam, *Applied Energy, 261* (2020), 114385.

[3] Ait Laasri, I., *et al*., Energy performance assessment of a novel enhanced solar thermal system with topology optimized latent heat thermal energy storage unit for domestic water heating, *Renewable Energy, 224* (2024), 120189.

[4] Chen, S., *et al*., Numerical investigation of form-stable composite phase change material for battery passive cooling, *Case Studies in Thermal Engineering, 50* (2023), 103410.

[5] Jiang, F., *et al*., Charging/discharging performance and corrosion behavior of a novel latent heat thermal energy storage device with different fin plate materials, *Renewable Energy, 220* (2024), 119584.

[6] Bahlekeh, A., *et al*., Evaluation of the solidification process in a double-tube latent heat storage unit equipped with circular fins with optimum fin spacing, *Energy Science & Engineering, 11* (2023), 7, pp. 2552–2570.

[7] Patel, J.R., *et al*., Influence of longitudinal fin arrangement on the melting and solidification inside the triplex tube latent heat thermal storage system, *Journal of Energy Storage, 46* (2022), 103778.

[8] Zhu, R., Jing, D., Numerical study on the discharging performance of a latent heat thermal energy storage system with fractal tree-shaped convergent fins, *Renewable Energy, 221* (2024), 119726.

[9] Rathod, M. K., Banerjee, J., Thermal performance enhancement of shell and tube Latent Heat Storage Unit using longitudinal fins, *Applied Thermal Engineering, 75* (2015), pp. 1084–1092.

[10] Yan, P., *et al*., Performance enhancement of phase change materials in triplex-tube latent heat energy storage system using novel fin configurations, *Applied Energy, 327* (2022), 120064.

[11] Zhang, Y., *et al*., Experimental investigation on the charging and discharging performance enhancement of a vertical latent heat thermal energy storage unit via snowflake fin design, *International Journal of Heat and Mass Transfer, 199* (2022), 123455.

[12] Boujelbene, M., *et al*., A comparative study of twisted and straight fins in enhancing the melting and solidifying rates of PCM in horizontal double-tube heat exchangers, *International Communications in Heat and Mass Transfer, 151* (2024), 107224.
[13] Mao, Q., *et al*., Heat Storage Performance of PCM in a Novel Vertical Pointer-Shaped Finned Latent Heat Tank, *Journal of Thermal Science, 33* (2024), 2, pp. 422–434.
[14] Nie, C., *et al*., Discharging performance evaluation and optimization of a latent heat thermal energy storage unit with helm-shaped fin, *Applied Thermal Engineering, 236* (2024), 121595.
[15] Yao, S., *et al*., Evaluation and Optimization of the Thermal Storage Performance of a Triplex-Tube Thermal Energy Storage System with V-Shaped Fins, *Journal of Thermal Science, 32* (2023), 6, pp. 2048–2064.
[16] Palmer, B., *et al*., Energy storage performance improvement of phase change materials-based triplex-tube heat exchanger (TTHX) using liquid-solid interface-informed fin configurations, *Applied Energy, 333* (2023), 120576.
[17] Tavakoli, A., *et al*., Physics-based modelling and data-driven optimisation of a latent heat thermal energy storage system with corrugated fins, *Renewable Energy, 217* (2023), 119200.
[18] Iranmanesh, A., A. Moshizi, S., Enhancing melting and solidification characteristics of a triple-pipe latent heat energy storage system via a wavy central wall with a sinusoidal fixed wavelength, *Journal of Energy Storage, 79* (2024), 110218.
[19] Kumar, A., *et al*., Transient analysis of PCM discharging in a rotary triplex tube with wave-shaped fins, *Journal of Energy Storage, 79* (2024), 110178.
[20] Guo, C., *et al*., Studying the advantages of equal curvature curved fin to enhance phase change heat storage, *Journal of Energy Storage, 57* (2023), 106212.
[21] Zaib, A., *et al*., Heat Transfer Augmentation Using Duplex and Triplex Tube Phase Change Material (PCM) Heat Exchanger Configurations, *Energies, 16* (2023), 10, 4037.
[22] Khedher, N.B., *et al*., Comprehensive analysis of melting enhancement by circular Y-shaped fins in a vertical shell-and-tube heat storage system, *Engineering Applications of Computational Fluid Mechanics, 17* (2023), 1, 2227682.
[23] Voller, V.R., Prakash, C., A fixed grid numerical modelling methodology for convection-diffusion mushy region phase-change problems, *International Journal of Heat and Mass Transfer, 30* (1987), pp. 1709–1719.
[24] Ebrahimi, A., *et al*., Sensitivity of Numerical Predictions to the Permeability Coefficient in Simulations of Melting and Solidification Using the Enthalpy-Porosity Method, *Energies, 12* (2019), 22, 4360.
[25] Al-Abidi, A.A., *et al*., Experimental study of melting and solidification of PCM in a triplex tube heat exchanger with fins, *Energy and Buildings, 68* (2014), pp. 33–41.

Submitted: 27.12.2024
Revised: 24.01.2025
Accepted: 28.01.2025